Nonlinear coupled axial–torsional vibration of single-walled carbon nanotubes using homotopy perturbation method

Alireza Fatahi-Vajari[1] ✉, *Zahra Azimzadeh*[2], *Muzamal Hussain*[3]

[1]*Department of Mechanical Engineering, Shahryar Branch, Islamic Azad University, Shahryar, Iran*
[2]*Department of Mathematics, Yadegar-e-Imam Khomeini (RAH) Shahr-e-Rey Branch, Islamic Azad University, Tehran, Iran*
[3]*Department of Mathematics, Government College University Faisalabad, 38040 Faisalabad, Pakistan*
✉ *E-mail: alirezafatahi@shriau.ac.ir*

Published in Micro & Nano Letters; Received on 29th March 2019; Revised on 6th August 2019; Accepted on 17th September 2019

This work analyses the nonlinear coupled axial–torsional vibration of single-walled carbon nanotubes (SWCNTs) based on numerical methods. Two-second order partial differential equations that govern the nonlinear coupled axial–torsional vibration for such nanotube are derived. First, these equations are reduced to ordinary differential equations using the Galerkin method and then solved using homotopy perturbation method (HPM) to obtain the nonlinear natural frequencies in coupled axial–torsional vibration mode. It is found that the obtained frequencies are complicated due to coupling between two vibration modes. The dependence of boundary conditions, vibration modes and nanotubes geometry on the nonlinear coupled axial–torsional vibration characteristics of SWCNTs are studied in detail. It was shown that boundary conditions and maximum initial vibration velocity have significant effects on the nonlinear coupled axial–torsional vibration response of SWCNTs. It was also seen that unlike the linear model if the maximum vibration velocity increases, the natural frequencies of vibration increases too. To show the effectiveness and ability of this method, the results obtained with HPM are compared with the fourth-order Runge-Kutta numerical results and good agreement is observed. To the knowledge of authors, the results given herein are new and can be used as a foundation work for future work.

1. Introduction: It is known that the mechanical behaviour of structures is divided into two general categories depending on whether the material phases are distributed continuously or discretely. If distribution is continuous, theories are based on classical continuum mechanics (CCM) and do not contain any scaling effects. This feature normally is the most important limitation of CCM [1, 2]. On account of nanoscale dimensions of carbon nanotubes (CNTs), it is hard to implement accurate experiments to obtain the properties of a CNT [3]. On the other hand, atomistic methods like molecular mechanics [4, 5] are costly and time-consuming to implement, especially for the systems having big dimensions.

To overcome the following limitations, various important modifications to CCM, known as higher-order gradient continuum theories were suggested to introduce microstructural features into the theory. One of the most important generalised continuum theories is the doublet mechanics theory, which was introduced by Granik and Ferrari [6] which assumes that the stress tensor at a given point is dependent to strains at all points of the continuum [7].

CNTs invented by Iijima in 1991 [8], have many exclusive and fascinating properties. With rapid development in nanotechnology, CNTs have great potential for wide applications as components in nano-electronic-mechanical systems which are receiving growing attention lately. The single-walled CNTs (SWCNTs) usually are subjected to complex and heavy dynamic loadings which have been caused by different sources. By producing different states of stress, these loads might result in excess vibrations and may lead to failure in some cases [9]. On the other hand, due to the excellent features and applications of CNTs, the precise prediction of the dynamic behaviour of such systems is essential. Two important forms of vibrations that have been identified for SWCNTs are axial and torsional vibrations. For example, for the flexible CNT with long distance between supports and high flexibility its torsional vibrations are much more significant. Furthermore, if the CNTs are presumed to be compressible, the axial vibration must be considered. Therefore, it is essential to consider the coupling effect between axial and torsional vibrations of SWCNTs, especially for studying stability conditions of CNTs. It can be seen from the previous works on the vibration of SWCNTs that most of existing SWCNTs systems have focused on the bending [9, 10], torsional [11–13], radial [14, 15], longitudinal [16, 17] or rotational [18, 19] vibrations behaviour of the shafts, solely and the coupling effect between the vibrational modes were ignored. The coupled vibration of SWCNTs is an interesting subject because of the complexity of the equations and the analytical solutions are difficult to obtain. One example is the coupling between axial–torsional vibrational behaviour of the SWCNT originated from the large deformation of the beam.

However, most of the researches on the axial and torsional vibration of CNTs have been limited to the linear theory, and the nonlinear regime is not considered yet. The homotopy perturbation method (HPM) is an efficient semi-analytical approach introduced by He [20, 21] for solving different linear and especially nonlinear engineering problems such as eigenvalue problems. In HPM, it is considered the solution as sum of a series with infinite terms. Usually, less than three sentences lead to good convergence and accuracy for the solution. The series used in HPM is different from Taylor series as it contains functions rather than terms in Taylor series. The method can be applied to a wide class of integral and differential equations; deterministic and stochastic problems; linear and nonlinear equations. The main advantages of this method to the other methods are simplicity, high convergence rate, more accurate results and time-saving especially in the non-homogeneous and nonlinear equations. The HPM was also applied to study nonlinear equations in science and engineering problems [22, 23].

To the best knowledge of authors, considering geometric nonlinearity effects along with the coupling of the axial–torsional vibrations on the dynamic behaviour of the SWCNTs is not studied yet and this Letter tries to consider such analysis. In other words, the main purpose of this study is to investigate and model a mechanism for the coupled nonlinear axial–torsional vibration of SWCNTs. Another goal of this Letter is to show the effectiveness of HPM and its ability in order at handling the nonlinear coupled torsional–axial vibration to obtain the nonlinear frequency equation.

doi: 10.1049/mnl.2019.0203

2. Basic equations of motion: The governing differential equations of motion for the coupled axial–torsional vibration of SWCNTs are derived in this section. Now, consider an SWCNT of mean radius R, length L, Young's modulus E, mass density ρ and Poisson's ratio ν as shown in Fig. 1.

In Fig. 1, r, θ, z are the orthogonal axes correspond to the normal, tangent and axial axes in cylindrical coordinates, respectively. The centre displacements of a given element along the axial, tangent and normal axes are shown by u_z, u_θ and u_r, respectively.

In the cylindrical coordinates, the equations of motion are [1, 24, 25]

$$\frac{\partial N_{zz}}{\partial z}+\frac{1}{r}\frac{\partial N_{\theta z}}{\partial \theta}+\rho f_z=\rho\frac{\partial^2 u_z}{\partial t^2} \tag{1}$$

$$\frac{\partial N_{z\theta}}{\partial z}+\frac{1}{r}\frac{\partial N_{\theta\theta}}{\partial \theta}+\frac{N_{\theta r}}{r}+\rho f_\theta=\rho\frac{\partial^2 u_\theta}{\partial t^2} \tag{2}$$

$$\frac{\partial N_{zr}}{\partial z}+\frac{1}{r}\frac{\partial N_{\theta r}}{\partial \theta}-\frac{N_{\theta\theta}}{r}+\rho f_r=\rho\frac{\partial^2 u_r}{\partial t^2} \tag{3}$$

$$\frac{\partial M_{zz}}{\partial z}+\frac{1}{r}\frac{\partial M_{\theta z}}{\partial \theta}+\rho\bar{l}_z=N_{zr} \tag{4}$$

$$\frac{\partial M_{z\theta}}{\partial z}+\frac{1}{r}\frac{\partial M_{\theta\theta}}{\partial \theta}+\frac{1}{r}M_{\theta r}+\rho\bar{l}_\theta=N_{\theta r} \tag{5}$$

$$\frac{M_{zr}}{\partial z}+\frac{1}{r}\frac{M_{\theta r}}{\partial \theta}-\frac{M_{\theta\theta}}{r}+\rho\bar{l}_r=N_{rr} \tag{6}$$

Equations (1)–(6) are the equations of motion in the cylindrical coordinates for a thin shell and should be solved to investigate the dynamic behaviour of the system. f_i and $\bar{l}_i$, $i\in\{1, 2, 3\}$ are body force and body moment, respectively. N_{ij} and M_{ij}, $i\in\{1, 2, 3\}, j\in\{1, 2, 3\}$ are resultant forces and resultant moments, respectively and are defined by the following equations:

$$N_{ij}=\int_{-(h/2)}^{h/2}\sigma_{ij}^{(M)}\mathrm{d}r,\quad M_{ij}=\int_{-(h/2)}^{h/2}z\sigma_{ij}^{(M)}\mathrm{d}r,\qquad i,j\in\{1, 2, 3\} \tag{7}$$

In this study, the following assumptions, known as Love's first approximation, for cylindrical shells are made [13, 14]:

(i) Any point that lies on a normal to middle plane remains same before and after the deformation. Thus, it is implied that the transverse shear stresses ($\sigma_{rz}^{(M)}$ and $\sigma_{r\theta}^{(M)}$) are presumed to be negligible.

(ii) Displacements in comparison with the thickness of the shell can be neglected.

(iii) It is assumed that the normal stresses ($\sigma_{rr}^{(M)}$) along the thickness direction is negligible.

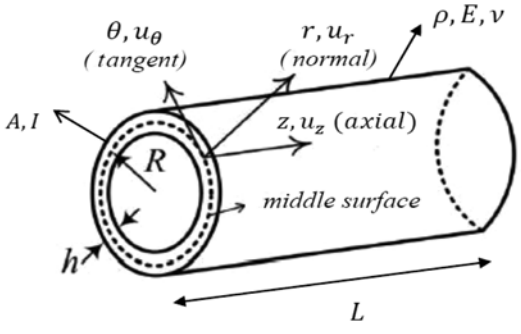

Fig. 1 *SWCNT in cylindrical coordinate*

It is further assumed that the nanotube is axisymmetric, homogeneous and vibrates in axial and torsional modes when the body forces are also neglected. From the later assumptions, it may be concluded

$$\frac{\partial}{\partial\theta}=\frac{\partial}{\partial r}=0,\quad u_r=0 \tag{8}$$

Under the above assumptions, (1)–(6) are reduced to the following equations:

$$\frac{\partial N_{zz}}{\partial z}=\rho\frac{\partial^2 u_z}{\partial t^2} \tag{9}$$

$$\frac{\partial N_{z\theta}}{\partial z}=\rho\frac{\partial^2 u_\theta}{\partial t^2} \tag{10}$$

which are the equations of motion for coupled torsional–axial vibration of SWCNTs. The nonlinear strain-displacement relation is written by [26]

$$\boldsymbol{\varepsilon}=\frac{1}{2}\left(\nabla\boldsymbol{u}+\nabla\boldsymbol{u}^{\mathrm{T}}+\nabla\boldsymbol{u}^{\mathrm{T}}\nabla\boldsymbol{u}\right) \tag{11}$$

where $\nabla\boldsymbol{u}$ can be written in cylindrical coordinate as

$$\nabla\boldsymbol{u}=\begin{bmatrix}\dfrac{\partial u_r}{\partial r} & \dfrac{1}{r}\left(\dfrac{\partial u_r}{\partial\theta}-u_\theta\right) & \dfrac{\partial u_r}{\partial z}\\ \dfrac{\partial u_\theta}{\partial r} & \dfrac{1}{r}\left(\dfrac{\partial u_\theta}{\partial\theta}+u_r\right) & \dfrac{\partial u_\theta}{\partial z}\\ \dfrac{\partial u_z}{\partial r} & \dfrac{1}{r}\dfrac{\partial u_z}{\partial\theta} & \dfrac{\partial u_z}{\partial z}\end{bmatrix} \tag{12}$$

Substituting (12) into (11) and making some manipulations, the following non-zero strain-displacement relations are obtained

$$\varepsilon_{z\theta}=\frac{1}{2}\left[2\frac{\partial u_\theta}{\partial z}+\frac{\partial u_\theta}{\partial z}\frac{\partial u_z}{\partial z}\right],\quad \varepsilon_{zz}=\frac{1}{2}\left[2\frac{\partial u_z}{\partial z}+\left(\frac{\partial u_\theta}{\partial z}\right)^2+\left(\frac{\partial u_z}{\partial z}\right)^2\right] \tag{13}$$

Substituting (13) into (9) and (10) with making some manipulations along with stress-strain relations, yields

$$Gh\left(\frac{\partial^2 u_\theta}{\partial z^2}+\frac{1}{2}\frac{\partial^2 u_\theta}{\partial z^2}\frac{\partial u_z}{\partial z}+\frac{1}{2}\frac{\partial u_\theta}{\partial z}\frac{\partial^2 u_z}{\partial z^2}\right)=\rho h\frac{\partial^2 u_\theta}{\partial t^2} \tag{14}$$

$$Eh\left(\frac{\partial^2 u_z}{\partial z^2}+\frac{\partial u_\theta}{\partial z}\frac{\partial^2 u_\theta}{\partial z^2}+\frac{\partial u_z}{\partial z}\frac{\partial^2 u_z}{\partial z^2}\right)=\rho h\frac{\partial^2 u_z}{\partial t^2} \tag{15}$$

Equations (14) and (15) are the equations of motion in nonlinear coupled vibration of SWCNTs. It can be seen that the two equations are coupled together. The corresponding linear governing equations can be simply obtained by setting the nonlinear terms to zero. In this case, the two equations will be decoupled.

3. Applying Galerkin and HPM to solve nonlinear governing equations: The nonlinear governing equations for the coupled axial–torsional vibration of SWCNTs are solved in this section. The nanotube is under the common boundary conditions listed in Table 1.

Now, the nonlinear equation of motion is solved to give the nonlinear frequency equation. Assuming $u_\theta(z, t)=\varphi(z)U(t)$ and $u_z(z, t)=\psi(z)W(t)$ where $\varphi(z)$ and $\psi(z)$ are the eigenmodes of the nanotube and satisfy the kinematic boundary conditions. $W(t)$ and $U(t)$ are the time-dependent parameters of the nanotube. The shape functions corresponding to the different boundary conditions are also given in Table 1.

Table 1 Common boundary conditions for the axial and torsional direction

Boundary conditions	Shape function	Governed condition at the boundaries
two clamped (C-C)	$\sin\left(\frac{n\pi}{L}z\right)$	$u = 0$ at $z = 0, L$
free-Free (F-F)	$\cos\left(\frac{n\pi}{L}z\right)$	$\frac{\partial u}{\partial z} = 0$ at $z = 0, L$
clamped-Free (C-F)	$1 - \cos\left(\frac{2n\pi}{L}z\right)$	$u = 0$ at $z = L$, $\frac{\partial u}{\partial z} = 0$ at $z = 0$

Applying the Galerkin method, the governing equations of motion ((14) and (15)) are reduced to the following ordinary differential equations:

$$G\left[a_1 U + \frac{1}{2}(a_2 + a_3)UW\right] = \rho a_4 \frac{\mathrm{d}^2 U}{\mathrm{d}t^2} \tag{16}$$

$$E\left[a_5 W + a_6 U^2 + a_7 W^2\right] = \rho a_8 \frac{\mathrm{d}^2 W}{\mathrm{d}t^2} \tag{17}$$

Equations (16) and (17) are under the initial conditions correspond to

$$U(0) = 0, \quad \frac{\mathrm{d}U}{\mathrm{d}t}(0) = U_{\max} \tag{18}$$

$$W(0) = 0, \quad \frac{\mathrm{d}W}{\mathrm{d}t}(0) = W_{\max} \tag{19}$$

where $U_{\max}$ and $W_{\max}$ denote the maximum initial velocities of vibration in circumferential and axial directions, respectively. In (16) and (17), a_1, a_1, ..., a_8 are given by the following relations:

$$\begin{aligned} \alpha_1 &= \int_0^L \varphi''(z)\varphi(z)\,\mathrm{d}z, \quad \alpha_2 = \int_0^L \varphi''(z)\psi'(z)\varphi(z)\,\mathrm{d}z, \\ \alpha_3 &= \int_0^L \varphi'(z)\psi''(x)\varphi(z)\,\mathrm{d}z, \quad \alpha_4 = \int_0^L \varphi^2(z)\,\mathrm{d}z \end{aligned} \tag{20}$$

$$\begin{aligned} \alpha_5 &= \int_0^L \psi''(z)\psi(z)\,\mathrm{d}z, \quad \alpha_6 = \int_0^L \varphi'(z)\varphi''(z)\psi(z)\,\mathrm{d}z, \\ \alpha_7 &= \int_0^L \varphi'(z)\psi''(z)\psi(z)\,\mathrm{d}z, \quad \alpha_8 = \int_0^L \psi^2(z)\,\mathrm{d}z \end{aligned} \tag{21}$$

After the following transformation $\tau = \omega t$, $\nu = \Omega t$, $a = U/r$, $b = W/r$ and $r = \sqrt{I/A}$, (16) and (17) are changed to the following nonlinear equations:

$$\omega^2 \frac{\mathrm{d}^2 a}{\mathrm{d}\tau^2} + Aa + Bab = 0 \tag{22}$$

$$\Omega^2 \frac{\mathrm{d}^2 b}{\mathrm{d}\nu^2} + Cb + Da^2 + Eb^2 = 0 \tag{23}$$

where ω and Ω are unknown nonlinear torsional and axial frequencies, respectively, in the coupled nonlinear torsional–axial vibration of SWCNTs that have to be determined. The coefficients A, B, C, D and E are also defined by the following relations:

$$A = -\frac{\alpha_1}{\alpha_4}\frac{G}{\rho} = \omega_L^2 \tag{24}$$

$$B = -\frac{1}{2}\frac{\alpha_2 + \alpha_3}{\alpha_4}\sqrt{\frac{I}{A}}\frac{G}{\rho} \tag{25}$$

$$C = -\frac{\alpha_5}{\alpha_8}\frac{E}{\rho} = \Omega_L^2 \tag{26}$$

$$D = -\frac{1}{2}\frac{\alpha_6}{\alpha_8}\sqrt{\frac{I}{A}}\frac{E}{\rho} \tag{27}$$

$$E = -\frac{1}{2}\frac{\alpha_7}{\alpha_8}\sqrt{\frac{I}{A}}\frac{E}{\rho} \tag{28}$$

In (24) and (26), $\omega_L = \sqrt{A}$ and $\Omega_L = \sqrt{C}$ are the linear frequencies in free vibration in the torsional and axial modes, respectively. To this end, new HPMs are created to seek the solutions of (22) and (23). The following homotopies with ω_0 and Ω_0 as the initial approximations for the frequencies are considered

$$(1-p)\omega_0^2\left(\frac{\mathrm{d}^2 a}{\mathrm{d}\tau^2} + a\right) + p\left(\omega^2\frac{\mathrm{d}^2 a}{\mathrm{d}\tau^2} + Aa + Bab\right) = 0 \tag{29}$$

$$(1-p)\Omega_0^2\left(\frac{\mathrm{d}^2 b}{\mathrm{d}\nu^2} + b\right) + p\left(\Omega^2\frac{\mathrm{d}^2 b}{\mathrm{d}\nu^2} + Cb + Da^2 + Eb^2\right) = 0 \tag{30}$$

Here p is a parameter, $a = a(\tau,\ p)$, $b = b(\nu,\ p)$, $\omega = \omega(p)$ and $\Omega = \Omega(p)$. Obviously, when $p = 0$, (29) and (30) give the following linear harmonic equations:

$$\frac{\mathrm{d}^2 a}{\mathrm{d}\tau^2} + a = 0, \quad a(0) = 0, \quad \frac{\mathrm{d}a(0)}{\mathrm{d}\tau} = X \tag{31}$$

$$\frac{\mathrm{d}^2 b}{\mathrm{d}\nu^2} + b = 0, \quad b(0) = 0, \quad \frac{\mathrm{d}b(0)}{\mathrm{d}\nu} = Y \tag{32}$$

where X and Y are defined by $X = U_{\max}/r\omega$ and $Y = W_{\max}/r\Omega$, respectively.

It is notable that for $p = 1$, (29) and (30) result the nonlinear (22) and (23), respectively. it can also be seen that as parameter p changes from 0 to 1, the solutions $a = a(\tau, p)$ and $\omega = \omega(p)$ along with $b = b(\nu, p)$, $\Omega = \Omega(p)$ of the homotopies (29) and (30) change from initial approximations $a_0(\tau)$, ω_0 and $b_0(\nu)$, Ω_0 to the required response $a(\tau)$, ω and $b(\nu)$, Ω of (22) and (23), respectively. Suppose the solutions of (22) and (23) to be in the following forms:

$$a(\tau) = a_0(\tau) + pa_1(\tau) + \ldots \tag{33}$$

$$\omega = \omega_0 + p\omega_1 + \ldots \tag{34}$$

$$b(\nu) = b_0(\nu) + pb_1(\nu) + \ldots \tag{35}$$

$$\Omega = \Omega_0 + p\Omega_1 + \ldots \tag{36}$$

Substituting the above relations into (29) and (30), respectively, and equalling the coefficients with equal powers of p in the terms, the following linear differential equations are obtained:

$$\begin{aligned} p^0&: \frac{d^2 a_0}{\partial\tau^2} + Aa_0 = 0,\ a_0(0) = 0,\ \frac{da_0(0)}{\partial\tau} = X \\ p^1&: \omega_0^2\left(\frac{d^2 a_1}{\partial\tau^2} + Aa_1\right) + \left(\omega^2\frac{d^2 a_0}{\partial\tau^2} + Aa_0 + Ba_0 b_0\right) \\ &= 0, \quad a_1(0) = 0, \quad \frac{da_1(0)}{\partial\tau} = 0 \\ &\vdots \end{aligned} \tag{37}$$

doi: 10.1049/mnl.2019.0203

$$
\begin{aligned}
&p^0: \frac{d^2 b_0}{\partial \nu^2} + A b_0 = 0, \quad b_0(0) = 0, \quad \frac{db_0(0)}{\partial \nu} = Y \\
&p^1: \Omega_0^2 \left(\frac{d^2 b_1}{\partial \nu^2} + A b_1 \right) + \left(\Omega^2 \frac{d^2 b_0}{\partial \nu^2} + C b_0 + D a_0^2 + E b_0^2 \right) \\
&\quad = 0, \quad b_1(0) = 0, \quad \frac{db_1(0)}{\partial \nu} = 0 \\
&\quad \vdots
\end{aligned} \tag{38}
$$

The initial approximation solutions of (37) and (38) are simply obtained by

$$a_0(\tau) = X \sin(\tau) \tag{39}$$

$$b_0(\nu) = Y \sin(\nu) \tag{40}$$

Substituting (39) and (40) into the first approximations of (37) and (38), respectively, it is obtained that

$$\omega_0^2 \left(\frac{\mathrm{d}^2 a_1}{\mathrm{d}\tau^2} + a_1 \right) + \left[-\omega_0^2 X \sin(\tau) + AX \sin(\tau) + BXY \sin^2(\tau) \right] = 0 \tag{41}$$

$$\begin{aligned}
\Omega_0^2 \left(\frac{\mathrm{d}^2 b_1}{\mathrm{d}\nu^2} + b_1 \right) + \left[-\Omega_0^2 Y \sin(\nu) + CY \sin(\nu) + DX^2 \sin^2(\nu) \right. \\
\left. + EY^2 \sin^2(\nu) \right] = 0
\end{aligned} \tag{42}$$

Expanding the trigonometric function using Fourier sine series for $\sin^2(\tau)$ in the first period yields

$$\sin^2(\tau) \cong \frac{8}{3\pi} \sin(\tau) - \frac{8}{15\pi} \sin(3\tau) \tag{43}$$

Substituting (43) into (41) and (42) and setting the coefficient of $\sin(\tau)$ to zero to eliminate the secular terms, it is found that

$$\omega = \sqrt{A + \frac{8}{3\pi} BY} \tag{44}$$

$$\Omega = \sqrt{C + \frac{8}{3\pi} \left(EY + D \frac{X^2}{Y} \right)} \tag{45}$$

It should be noted that if it is set as $B = 0$ in (44) and also $D = E = 0$ in (45), the obtaining results are in complete agreement with those obtained using the linear method presented in [11, 18].

From (44) and (45), it can be concluded that unlike the linear systems, the frequencies are dependent on vibration velocities related to the initial conditions. As the vibration velocities increase, the nonlinear frequencies increase too and thus the discrepancy between the linear and nonlinear frequencies become significant. It should be noted that if the dependence of the frequency to vibration velocity is neglected, the linear frequencies are obtained. The results demonstrate that the nonlinear torsional frequency is different from the linear part only by addition of the torsional initial vibrations velocity but the nonlinear axial frequency is dependent on the torsional and axial initial vibration velocities of the system.

Considering (44) and (45), the solutions of (41) and (42) can be obtained as

$$a_1(\tau) = \frac{3}{5} \frac{BXY}{3\pi A + 8BX} \left[\sin(\tau) - \frac{1}{3} \sin(3\tau) \right] \tag{46}$$

$$b_1(\nu) = \frac{3}{5} \frac{EY^2 + DX^2}{3\pi YC + 8\left(EY^2 + DX^2\right)} \left[\sin(\nu) - \frac{1}{3} \sin(3\nu) \right] \tag{47}$$

Thus, the first approximate solution of (22) and (23) is written by the following equations:

$$\begin{aligned}
a(\tau) &= a_0(\tau) + a_1(\tau) \\
&= X \sin(\tau) + \frac{3}{5} \frac{BXY}{3\pi A + 8BX} \left[\sin(\tau) - \frac{1}{3} \sin(3\tau) \right]
\end{aligned} \tag{48}$$

$$\begin{aligned}
b(\nu) &= b_0(\nu) + b_1(\nu) \\
&= Y \sin(\nu) + \frac{3}{5} \frac{EY^2 + DX^2}{3\pi YC + 8\left(EY^2 + DX^2\right)} \left[\sin(\nu) - \frac{1}{3} \sin(3\nu) \right]
\end{aligned} \tag{49}$$

4. Results and discussion: To validate the presented method, the results obtained herein using Galerkin and HPM methods are compared with the available numerical results.

To this end, in Fig. 2 non-dimensional amplitude of vibration for axial and torsional modes are drawn against the non-dimensional time using the fourth-order Runge-Kutta method and the presented method. The sample SWCNT that has been used in this figure and upcoming figures is Zigzag (16, 0) with clamped-free (C-F) boundary condition. From this figure, it can be seen that the results of the present method are in good agreement with the forth-ordered Runge-Kutta numerical results. Now, the dependence of boundary conditions, vibration modes and nanotubes geometry on the nonlinear coupled axial–torsional vibration characteristics of SWCNTs are studied in detail for Zigzag (16, 0). It should be added that one may relate the natural frequency (f) to the angular frequency (ω) as $f = w/2\pi$. This equation is used in Figs. 3–6 to give the frequencies in THz. Throughout this Letter, the mechanical properties of SWCNT are assumed to be: Poisson's ratio $\nu = 0.2$, mass density $\rho = 2300\,(\mathrm{kg/m^3})$ and Young's modulus $E = 1.1$ TPa [1].

Figs. 3 and 4 show the nonlinear natural frequencies variation versus maximum torsional and axial vibration velocities, respectively. As can be seen from these figures, unlike the linear one, the nonlinear frequencies are dependent to the maximum vibration velocity so that the larger the velocity, the discrepancy between the linear and nonlinear frequencies becomes bigger. In Fig. 3, as the non-dimensional maximum torsional vibration velocity increases, the nonlinear axial natural frequency increases too while nonlinear torsional frequency becomes constant. It means that in coupled nonlinear vibration of CNTs, the nonlinear torsional natural frequency is independent to maximum torsional vibration velocity.

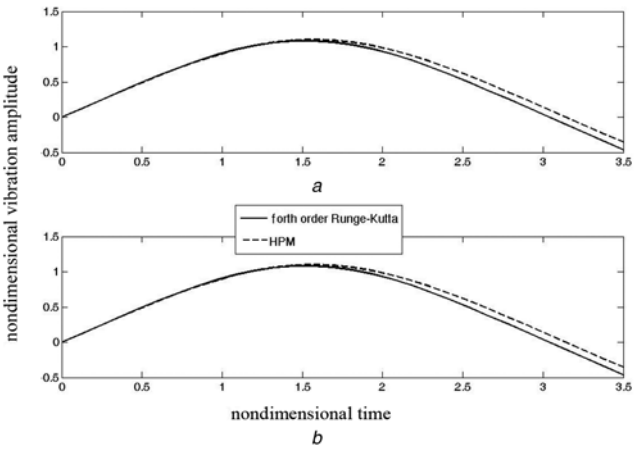

Fig. 2 *Non-dimensional vibration amplitudes*
a for torsional and
b for axial vibration; *a* and *b* versus non-dimensional time for $X = 1$

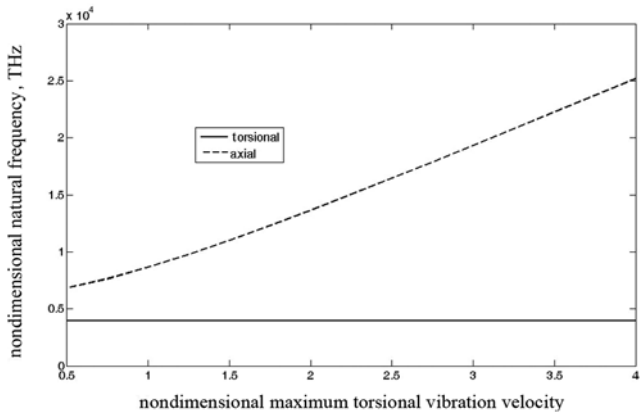

Fig. 3 *Nonlinear natural frequencies versus non-dimensional maximum vibration velocity in torsional mode with* $X = 1$

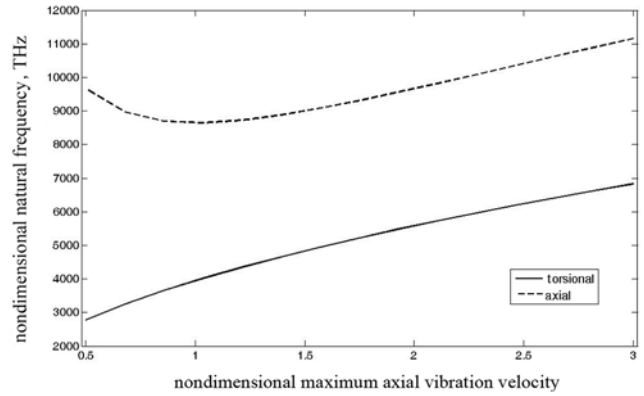

Fig. 4 *Nonlinear natural frequencies versus non-dimensional maximum axial vibration velocity with* $X = 1$

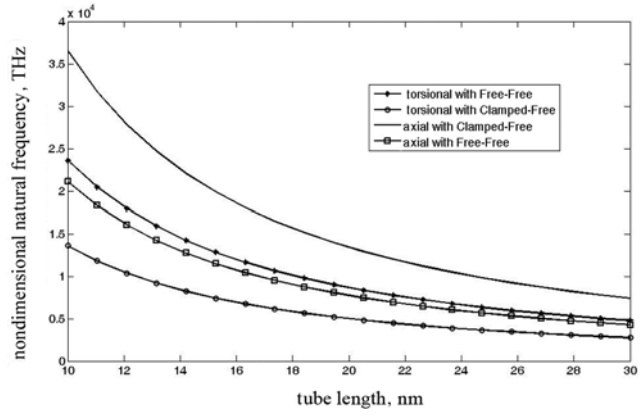

Fig. 5 *Nonlinear natural frequencies versus tube length with* $X = 1$ *and* $Y = 1$ *with different boundaries*

In Fig. 4, it can be seen that if the non-dimensional maximum axial vibration velocity increases, the nonlinear torsional natural frequency increases too. While there is a minimum point in the nonlinear axial natural frequency curve. This minimum can be obtained by differentiating nonlinear axial natural frequency with respect to non-dimensional maximum axial vibration velocity.

The nonlinear natural frequencies versus tube length are plotted in Fig. 5 under free-free (F-F) and C-F boundary conditions. It can be seen that as the length of the tube increases, the nonlinear natural frequencies of SWCNTs decrease. This decreasing is more evident for lower tube lengths. As it is expected, the clamped boundary condition has the highest natural frequency in comparison with the other boundaries. It can also be seen that as the tube length increases, the nonlinear frequencies approach the linear ones, especially for higher lengths. It can also be seen that in the same conditions, nonlinear axial natural frequency is much higher than the torsional one. This discrepancy is more apparent in lower lengths. In Fig. 6, nonlinear frequencies have been plotted against tube diameter for various vibration modes. From this figure, it is seen that as the diameter of the tube increases, the nonlinear frequencies increase, too. This increase is more significant in higher vibration modes and also for higher tube diameter. It is also seen that as the vibration mode increases, the nonlinear frequency increases too.

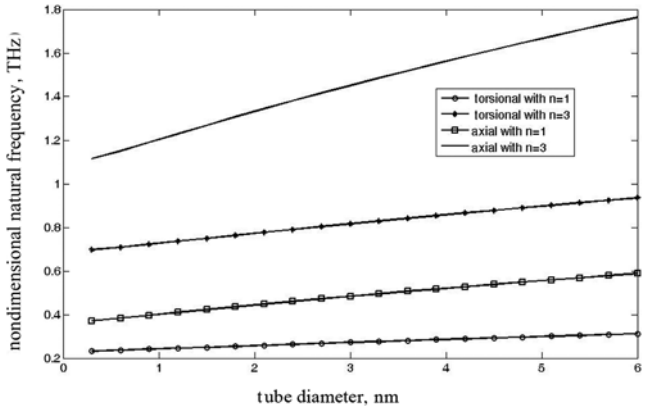

Fig. 6 *Nonlinear natural frequencies with tube diameter with* $X = 1$ *and* $Y = 1$ *for different vibration modes*

5. Conclusions: The nonlinear coupled torsional–axial vibration of SWCNTs based on Galerkin and HPM has been investigated in this study. The equations of motion for nonlinear coupled torsional–axial vibration of the SWCNT are derived and solved to give the frequency equations in coupled torsional–axial mode with arbitrary end conditions. The significant dependence of these frequencies to tube diameter, tube length and the maximum vibration velocity are investigated in various boundary conditions and vibration modes. To validate the accuracy and ability of the present method, the calculated results were compared with numerical results and good agreement has been obtained. The following notes are especially concluded in this study.

(i) Owing to the coupling between the torsional and axial vibrations, axial and torsional nonlinear frequencies are defined in this study. If the nonlinear terms of velocity in frequencies are neglected, the linear natural frequencies are obtained in which the axial and torsional vibrations are decoupled.

(ii) Owing to nonlinear nature of the equations, the calculated frequencies are dependent to the maximum axial and torsional vibration velocities.

(iii) The coupling between the axial and torsional vibrations is due to the existence of large deformation terms in the nonlinear governing equations of the system. The nonlinearity effects lead to increase in the frequencies comparing with the linear model.

(iv) The natural frequencies increase if the end conditions change from C-F through to fully clamped, denoted by C-C. This effect is more apparent for lower tube lengths.

doi: 10.1049/mnl.2019.0203

(v) For the same maximum vibration velocity and also tube length/diameter, the axial frequency is higher than the torsional one. This difference is more evident in higher vibration modes and lower lengths.

(vi) As the length of the tube increases, the frequencies decrease. This decreasing is more apparent in clamped boundary condition and higher vibration mode. From this, it is implied that with an increase in the tube length, the interaction of the axial and torsional vibrations decreases. However, with increasing the tube diameter, an inverse effect is seen.

6 References

[1] Fatahi-Vajari A.: 'A new method for evaluating the natural frequency in radial breathing like mode vibration of double-walled carbon nanotubes', *Zeitschrift für Angewandte Mathematik und Mechanik.*, 2018, **98**, (2), pp. 255–269

[2] Ferrari M., Granik V.T., Imam A., *ET AL.*: 'Advances in doublet mechanics' (Springer, Berlin, 1997)

[3] Bachilo S.M., Strano M.S., Kittrell C., *ET AL.*: 'Structure-assigned optical spectra of single-walled carbon nanotubes', *Science.*, 2002, **298**, pp. 2361–2366

[4] Gupta S.S., Batra R.C.: 'Continuum structures equivalent in normal mode vibrations to single-walled carbon nanotubes', *Comput. Mater. Sci..*, 2008, **43**, pp. 715–723

[5] Gupta S.S., Bosco F.G., Batra R.C.: 'Wall thickness and elastic moduli of single-walled carbon nanotubes from frequencies of torsional, torsional and in extensional modes of vibration', *Comput. Mater. Sci..*, 2010, **47**, pp. 1049–1059

[6] Granik V.T., Ferrari M.: 'Microstructural mechanics of granular media', *Mech. Mater..*, 1993, **15**, pp. 301–322

[7] Azimzadeh Z., Fatahi-Vajari A.: 'Coupled axial-radial vibration of single-walled carbon nanotubes via doublet mechanics', *J. Solid Mechanics.*, 2019, **11**, (2), pp. 323–340

[8] Iijima S.: 'Helical microtubes of graphitic carbon', *Nature (London).*, 1991, **354**, pp. 56–58

[9] Fatahi-Vajari A., Imam A.: 'Lateral vibration of single-layered graphine sheets using doublet mechanics', *J. Solid Mechanics.*, 2016, **8**, (4), pp. 875–894

[10] Bocko J., Lengvarský P.: 'Bending vibrations of carbon nanotubes by using nonlocal theory', *Procedia Eng..*, 2014, **96**, pp. 21–27

[11] Fatahi-Vajari A., Imam A.: 'Torsional vibration of single-walled carbon nanotubes using doublet mechanics', *Zeitschrift für Angewandte Mathematik und Physik*, 2016, **67**, pp. 1–22

[12] Arda M., Aydogdu M.: 'Analysis of free torsional vibration in carbon nanotubes embedded in a viscoelastic medium', *Adv. Sci. Technol. Res. J.*, 2015, **9**, (26), pp. 28–33

[13] Selim M.M.: 'Torsional vibration of carbon nanotubes under initial compression stress', *Braz. J. Phys..*, 2009, **40**, (3), pp. 283–287

[14] Fatahi-Vajari A., Imam A.: 'Analysis of radial breathing mode of vibration of single-walled carbon nanotubes via doublet mechanics', *Zeitschrift für Angewandte Mathematik und Mechanik.*, 2016, **96**, (9), pp. 1020–1032

[15] Liand Q.M., Shi M.X.: 'Intermittent transformation between radial breathing and flexural vibration modes in a single-walled carbon nanotube', *Proc. R. Soc. A.*, 2008, **464**, pp. 1941–1953

[16] Fatahi-Vajari A., Imam A.: 'Axial vibration of single-walled carbon nanotubes using doublet mechanics', *Indian J. Phys..*, 2016, **90**, (4), pp. 447–455

[17] Aydogdu M.: 'Axial vibration analysis of nanorods (carbon nanotubes) embedded in an elastic medium using nonlocal elasticity', *Mech. Res. Commun.*, 2012, **43**, pp. 34–40

[18] Hussain M., Naeem M.N., Taj M.: 'Vibration characteristics of zigzag and chiral FGM rotating carbon nanotubes sandwich with ring supports', *J. Mechanical Eng. Sci. C.*, 2019, **233**, (16), pp. 5763–5780, DOI: 10.1177/0954406219855095

[19] Hussain M., Naeem M.N., Shahzad A., *ET AL.*: 'Vibrations of rotating cylindrical shells with FGM using wave propagation approach', *IMEchE Part C: J. Mechanical Eng. Sci.*, 2018, **232**, (23), pp. 4342–4356

[20] He J.H.: 'Approximate analytical solution for seepage flow with fractional derivatives in porous media', *Comput. Methods Appl. Mech. Eng..*, 1998, **167**, pp. 57–68

[21] He J.H.: 'Homotopy perturbation method for solving boundary value problems', *Phys. Lett., Section A.*, 2006, **350**, (1–2), pp. 87–88

[22] Azimzadeh Z., Vahidi A.R., Babolian E.: 'Exact solutions for nonlinear Duffing's equations by He's homotopy perturbation method', *Indian J. Phys..*, 2012, **86**, (8), pp. 721–726

[23] Ghasemi M., Tavassoli Kajani M., Davari A.: 'Numerical solution of two dimensional nonlinear differential equation by homotopy perturbation method', *Appl. Math. Comput..*, 2007, **189**, pp. 341–345

[24] Hussain M., Naeem M.N.: 'Vibration analysis of single-walled carbon nanotubes using wave propagation approach', *Mechanical Sci.*, 2017, **8**, (1), pp. 155–164

[25] Hussain M., Naeem M.N., Shahzad A., *ET AL.*: 'Vibrational behavior of single-walled carbon nanotubes based on cylindrical shell model using wave propagation approach', *AIP Adv.*, 2017, **7**, (4), p. 045114

[26] Boresi A.P., Chong K.P.: 'Elasticity in engineering mechanics' (John Wiley and Sons, New York, 2000)